

# Investigation of Composite Behaviour of Lath Martensite

János Endre MARÓTI,<sup>1</sup> Péter János SZABÓ<sup>2</sup>

*Budapest University of Technology and Economics, Faculty of Mechanical Engineering, Department of Materials Science and Engineering, Budapest, Hungary*

<sup>1</sup> maroti@eik.bme.hu

<sup>2</sup> szpj@eik.bme.hu

## Abstract

It is very important for our research that we are able to examine the orientation of packets and their relationship to directions of stress that cause plastic deformation. We use electron backscatter diffraction (EBSD) to achieve this. EBSD examination requires very careful sample preparation. In our work we have developed a sample preparation method for electron backscatter diffraction examination. In this study we present the method, which consists of multistage mechanical grinding, polishing and ion polishing. Optimal parameters for each steps (eg.: grinding, polishing and sputtering time, milling angle) were determined for lath martensitic steel, however, it could be used for other type of steel with minor adjustments.

**Keywords:** austenite, martensite, EBSD, sample preparation.

## 1. Introduction

Martensitic steel is one of the most widely used iron base structural materials with the most outstanding mechanical properties. Besides Fe it consists of carbon varying between a few hundredths to a few tenths of a percent by weight and a variety of different alloying elements in small quantities. It is produced by fast cooling from a temperature where the fcc austenitic  $\gamma$  phase is stable to around room temperature, where the bcc  $\alpha$  phase is stable. All physical properties depend on the alloy composition, but principally on carbon content and cooling characteristics. The speed of cooling from the austenite state and the carbon content are the main factors determining the microstructure and the mechanical properties of martensitic steels [1].

One possible form of martensite is the so called lath martensite. A typical lath martensite consists of blocks of lamellar plates where the blocks form packets [2–4]. The blocks are further subdivided into sub-blocks, where the smallest constituents of the structure are the lamellar plates called martensite-laths. The hierarchical structure of packets, blocks, sub-blocks and laths in lath martensite is shown schematically in Figure 1.

Within the prior austenite grain boundary several packets of different crystallographic orientations can coexist [2–4], as shown in Figure 1.

Despite the rather large elastic limit of martensitic steels they do show some ductility [1, 5–7]. There have recently been attempts to reveal the microscopic mechanism controlling plastic deformation in lath-martensite, by microscale deformation experiments [8–9].

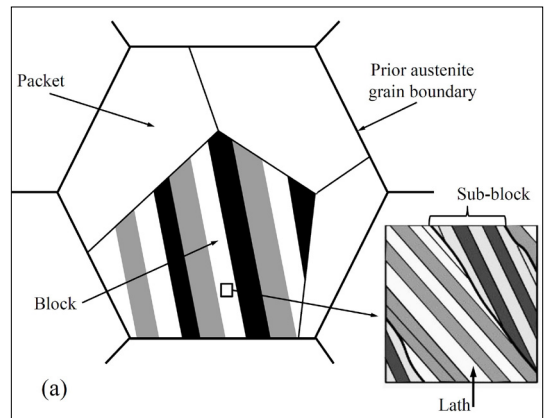


**Figure 1.** The hierarchical structure of packets, sub-blocks, blocks and lath in lath martensite.

Micropillars with a single martensite block have shown perfectly ideal stress-strain behaviour with no strain hardening and a flow stress of 1.2 GPa. Micropillars with two or more blocks, however, have shown significant strain hardening with a similarly large elastic limit [8].

Tensile experiments on microscale specimens of lath martensite of the order of 100  $\mu\text{m}$  length showed that the critical-resolved-shear-stress (CRSS) was relatively small, of the order of 350 MPa, when the active slip systems were in-lath-plane, whereas the CRSS was almost doubled when the active slip systems were out-of-lath-plane [9].

The two experiments in [8, 9] indicate that there may be a load redistribution between packets in which the active slip systems are in- or out-of-lath-plane. Two packets oriented with the active Burgers vectors either in- or out-of-lath-plane relative to the direction of the applied stress,  $\sigma$ , are shown schematically in Figure 2.

The different elastic-plastic response is brought about solely by the different crystallographic orientation of the two packets relative to the direction of  $\sigma$ . As a result, the plastic deformation creates a composite in which the packets with active Burgers vectors in-lath-plane become the soft, whereas those with active Burgers vectors out-of-lath-plane become the hard components.

This short introduction shows how important it is for our research that we are able to examine the orientation of packets and those relationships with directions of stress which cause of plastic deformation. We use electron backscatter diffraction (EBSD) to achieve this. EBSD examination requires very careful sample preparation. In our

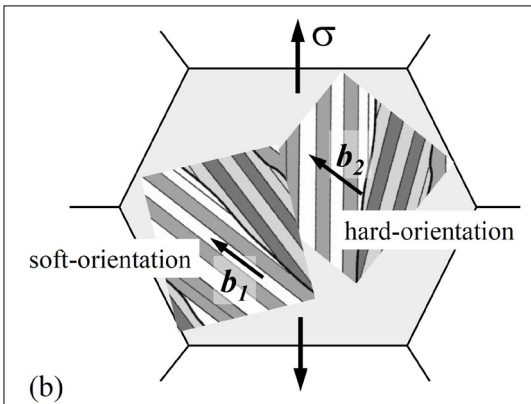


**Figure 2.** Two packets oriented with the active Burgers vectors either in- or out-of-lath plane relative to the direction of the applied stress

work we have developed a sample preparation method for electron backscatter diffraction examination.

## 2. Materials and methods

The samples were used for our measurements with edge lengths of  $l_1 = 20 \text{ mm}$  and  $l_2 = 20 \text{ mm}$  and a thickness of  $h = 2.5 \text{ mm}$ . The material composition of the specimens is summarized in Table 1. The material composition of the specimens was measured using a Zeiss Evo MA 10 Scanning Electron Microscope (SEM).

The samples were heated to 1100  $^{\circ}\text{C}$  (this is above the temperature of steel A3) and then held for 30 min followed by water cooling down to 20  $^{\circ}\text{C}$ . This way, we could produce lath martensite.

In the next step, the specimens were embedded in an electrically conductive hot embedding resin. This is an important step because both EBSD and ion polisher can examine well only conductive samples, so there is no need to take out the specimens from the resin and risk them in this way possible injuries.

The next step was mechanical grinding and polishing with different Silicon carbide (SiC) and diamond particle size sandpapers (SiC particle sizes: 300  $\mu\text{m}$ , 212  $\mu\text{m}$ , 90  $\mu\text{m}$ , 46  $\mu\text{m}$ , 26  $\mu\text{m}$ , 15  $\mu\text{m}$ , 12  $\mu\text{m}$ , 6  $\mu\text{m}$ ; diamond particle sizes: 3  $\mu\text{m}$ , 1  $\mu\text{m}$ ). All types of grinding paper were used for 5 minutes and all types of polishing paper were used for 10 minutes. At this point, all of the specimens were prepared in the same way, but this is insufficient for EBSD measurements. For better results, the specimens were ionpolished with a Technoorg Linda SEM Prep2 ionpolisher. The task may seem easy at first, but accurate adjustment of many variables (anode voltage, anode current, milling angle, sputtering time, ion source) is required for proper sample preparation. Two of the variables were changed during the measurement, one of them – the milling angle – was changed from 10 to 110, the other variable was the sputter time, this was increased from 1 hour to 6 hours.

**Table 1.** Material composition of our specimens.

Element	Weight %
Fe	98.10
C	0.21
Mn	1.58
P	0.03
S	0.04
Si	0.04

The other variables were set to the following values: anode voltage: 10 kV, anode current: 3.5 A, beam current: 2 mA, ion: Ar<sup>+</sup>.

After the samples were prepared, we performed EBSD measurements. From the measurements, we obtain IQ (image quality) maps which are used to determine the quality of image from electron backscattered diffraction examination.

The higher the IQ value, the better the obtained result. Our goal is that the IQ value exceeds 40,000 because the results obtained above this are already correct.

### 3. Results

First, we established the ideal milling angle. Each sample was ionpolished for 1 hour. The IQ values for each milling angle were plotted in the following diagram (Figure 3).

As we can see in the diagram, the ideal milling angle is 70. After this, only the sputter time was modified and the milling angle was set at 70. The result can be seen in the Figure 4.

As we can see in the diagram, the ideal sputtering time was 4 hours, but the average IQ value was over 40000 at 3 and 5 hours. Based on this, we can say the best ion polishing parameters are:

- anode voltage: 10 kV,
- anode current: 3.5 A,
- beam current: 2 mA,
- ion: Ar<sup>+</sup>,
- sputtering time: 4 h,
- milling angle: 7°.

An IQ map of a sample made with these parameters in Figure 5.

### Acknowledgement

The publication of the work reported herein has been supported by the NTP-SZKOLL-19-066 National Talent Programme of the Ministry of Human Capacities, and by the „OTKA” grant K124926 funded by National Research, Development and Innovation Office (NKFIH).

### References

- [1] Krauss G.: *Martensite in steel: strength and structure*. Material Science and Engineering A, 273-275. (1999) 40–57.  
[https://doi.org/10.1016/S0921-5093\(99\)00288-9](https://doi.org/10.1016/S0921-5093(99)00288-9)
- [2] Krauss G., Mader A. R.: *The morphology of martensite in iron alloys*. Metallurgical Transactions, 2. (1971) 2343–2357.  
<https://doi.org/10.1007/BF02814873>
- [3] Morito S., Tanaka H., Konishi R., Furuhashi T., Maki T.: *The morphology and crystallography of lath martensite in Fe-C alloys*. Acta Materialia, 51. (2003) 1789–1799.  
[https://doi.org/10.1016/S1359-6454\(02\)00577-3](https://doi.org/10.1016/S1359-6454(02)00577-3)



**Figure 3.** Average IQ values of EBSD measurement of our steel specimens as a function of the milling angle of the samples, where the sputtering time was 1 hour.

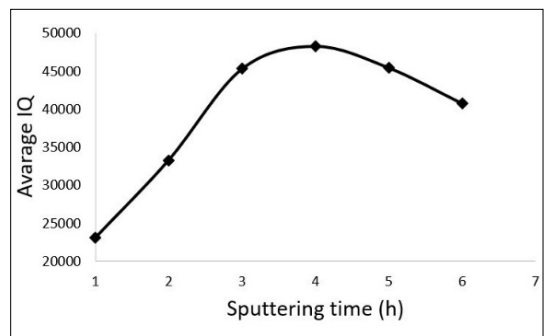


**Figure 4.** Average IQ values of EBSD measurement of our steel specimens as a function of the sputtering time of the samples, where the milling angle was 7°.

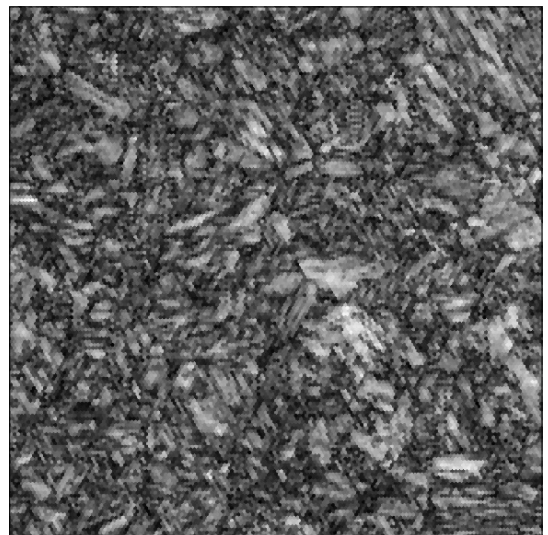


**Figure 5.** IQ map of a sample made with best parameters.

- [4] Kitahara H., Ueji R., Tsuji N., Minamino Y.: *Crystallographic features of lath martensite in low-carbon steel*. Acta Materialia, 54. (2006) 1279–1288. <https://doi.org/10.1016/j.actamat.2005.11.001>
- [5] Swarr T., Krauss G.: *The effect of structure on the deformation of as-wuenced and tempered martensite in an Fe-0.2 pct C alloy*. Metallurgical Transactions A, 7/1. (1976) 41–48. <https://doi.org/10.1007/BF02644037>
- [6] Michiuchi M., Nambu S., Ishimoto Y., Inoue J., Koseki, T.: *Relationship between local deformation behavior and crystallographic features of as-quenched lath martensite during uniaxial tensile deformation*. Acta Materialia, 57. (2009) 5283–5291. <https://doi.org/10.1016/j.actamat.2009.06.021>
- [7] Nambu S., Michiuchi M., Ishimoto Y., Asakura K., Inoue J., Koseki T.: *Transition in deformation behaviour of martensitic steel during large deformation under uniaxial tensile loading*. Scripta Materialia, 60. (2009) 221–224. <https://doi.org/10.1016/j.scriptamat.2008.10.07>
- [8] Ghassemi-Armaki H., Chen P., Bhat S., Sadagopan S. Kumar S., Bower A.: *Microscale-calibrated modeling of the deformation response of low-carbon martensite*. Acta Materialia, 61. (2013) 640–662. <https://doi.org/10.1016/j.actamat.2013.10.001>
- [9] Mine Y., Hirashita K., Takashima H., Matsuda M., Takashima K.: *Micro-tension behaviour of lath martensite structures of carbon steel*. Material Science and Engineering A, (2013) 535–544. <https://doi.org/10.1016/j.msea.2012.09.099>